Optical Absorption and Structural Properties of as-deposited and Thermally Annealed As-Te-Ga Thin Films

M. Dongol

Physics Department, Faculty of Science, South Valley University, Qena , Egypt

Thin films of As_{30} Te_{70-x} Ga_x, where x = 0.5, 1, 3, 6 and 10 are deposited on glass substrates by vacuum evaporation. The transmittance and absorbance of the as-deposited films were measured in the spectral range 400-1100nm. The dependence of the absorption coefficient on the photon energy is well described by the relation $\alpha h\nu = B (h\nu - E_0)^2$. The optical energy is nearly independent on the Ga content up to 3 at.% , then increases continuously from 0.73 eV to 0.9eV with increasing the Ga content. Thermal annealing below and above the glass transition temperature slightly increase and decrease the value of the optical energy gap, respectively. XRD, SAED, TEM and DSC were used to study the structure of the as-deposited and annealed films. The amount and type of the separated polycrystalline phases depend on the original composition of the film and on the annealing temperature.

Introduction:

The study of the optical constants of a material is interesting for many reasons. Firstly, the use of materials in optical applications such as interference filters, optical fibers, and reflective coating requires accurate knowledge of their optical constants over a wide range of wavelengths. Secondly, the optical properties of all materials may be related to their atomic structure, electronic band structure and electrical properties. Thus, the study of the optical constants, enable correlation to be made with the band structures derived by other methods.

The optical and electrical properties of chalcogenide glasses are generally much less sensitive to nonstoichiometry and the presence of impurities is less sensitive than crystalline semiconductors. This common insensitivity has been explained by Mott[1], who postulated that the impurities are coordinated in keeping with the(8-N) rule such that their covalent bonding requirements are satisfying. As a result, such impurities are not expected to form distinct absorption centers or impurity levels in the mobility gap but would only contribute to the fluctuation of the internal potential.

In this paper a series of systematic investigations on the structural and optical properties of As_{30} Te_{70-x} Ga_x (where x = 0.5, 1, 3, 6 and 10) are reported. The dependence of the optical transition on the Ga content is investigated. Also, the effect of thermal annealing on the optical properties and the structure are given.

The results has been discussed on the basis of thermally induced transformations, of new charged centers C_3 and $Ga(C_2)_3$ in the mobility gap.

Experimental:

Thin films of the As_{30} Te_{70-x} Ga_x, (where x = 0.5, 1, 3, 6 and 10) have been prepared using Coating system Edward E306 operated at 5×10^{-6} Torr. The chosen compositions lie in the vitreios region determined by Dunaev et al. [2] as shown in Fig. (1). The deposition of thin films was carried out onto ultrasonically cleaned glass substrates kept at room temperature. A quartz crystal monitor Edward FTM5 was used to control the film thickness as well as the deposition rate. All the investigated films were deposited under the same conditions to follow up the compositional dependence and annealing temperature of the optical properties of the As_{30} Te_{70-x} Ga_x films.

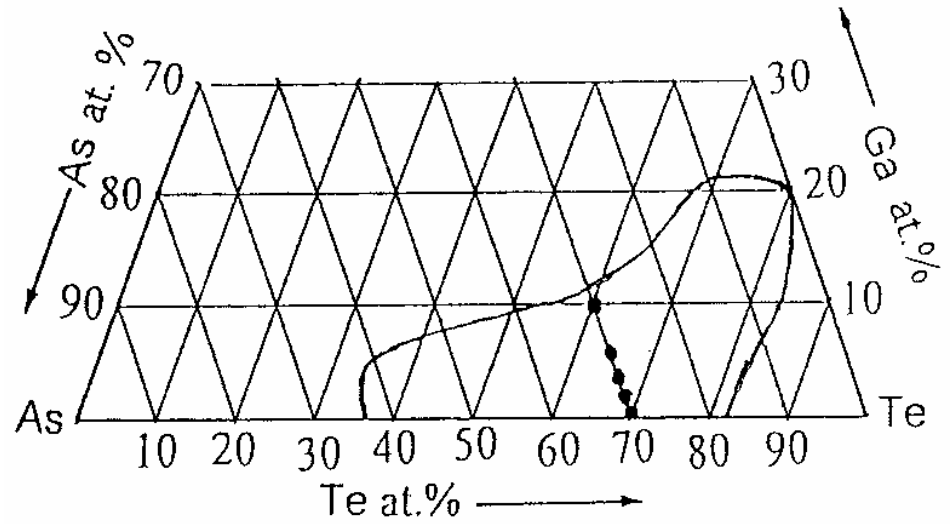

Fig.(1): The glass formation region of glass formation in As-Te-Ga system. The compositions of the as-prepared As-Te-Ga glasses of the present work are shown in the figure.

X-ray diffraction (XRD) analysis was performed using Philips diffractometer (type 1710) using Cu-Kα radiation, λ=1.5418 Å, operated at 40 kV and 30 mA, with a scanning speed of 3.76 deg/min. All measurements were carried out at room temperature. Energy dispersive X-ray spectroscopy (Link Analytical EDX) was used to measure the elemental composition of the investigated films.

The thermal behaviour was measured using differential scanning calorimeter (DSC) in a thermal analysis system (Shimadzu Ta-50). The powdered sample (25-30 mg) was heated in an aluminum pan at a heating rate of 10 K/min.

The optical transmittance (T) and absorbance (A) of the deposited thin films were measured at normal incidence at room temperature using a double UV-VIS scanning spectrophotometer (Shimadzu) in the wavelength range 200-1100 nm. Heat treatment for $As_{30}Te_{70-x}Ga_x$ films was performed under a flow of a nitrogen gas.

Results and Discussion:

The composition of the as-deposited As_{30} Te_{70-x} Ga_x films was investigated using EDX technique and the computed atomic percentage ratios of the As, Te, and Ga are very close to the bulk compositions . Deviations of the constituents elements did not exceed 1.0 at%.

Figure (2) shows DSC thermograms for powdered $As_{30}Te_{67}Ga_3$ $As_{30}Te_{46}Ga_6$ chalcogenide glasses. The general features of DSC thermograms (glass transition temperature T_g, and crystallization peaks T_p) were determined and reported in Table (1). It is noticed that both T_g and T_p increase with increasing Ga content.

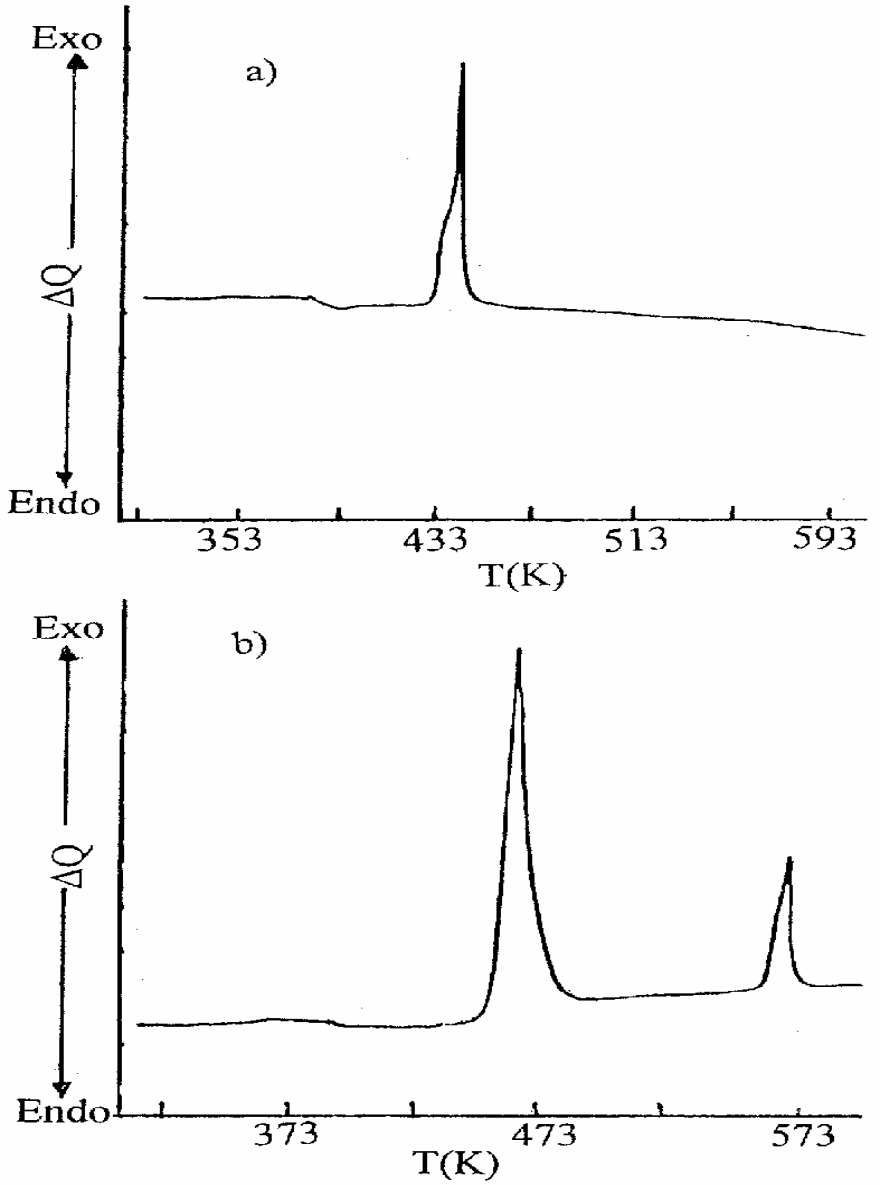

Fig.(2): DSC thermograms for powdered:
(a) As_{30} Te_{67} Ga_3 chalcogenide glass.
(b) As_{30} Te_{64} Ca_6 chalcogenide glass.

Table (1): The glass transition temperature T_g and the crystallization temperatures T_p at different values of Ga content.

Ga (at.%)	T_g (K)	T_{p1} (K)	T_{p2} (K)
1	376	436	---
3	383	441	455
6	390	463	572
10	404	491	----

The X-ray diffraction patterns for the as-deposited $As_{30}Te_{70-x}Ga_x$ films are shown in Fig. (3). The diffraction does not show any peaks, indicating that all the as- deposted films containing Ga up to 10 at.%, were amorphous. The films were crystallized by annealing at temperature of 423K for 2 hr. (which is close to their T_p, as obtained from DSC analysis).The X-ray patterns of a typical $As_{30}Te_{67}Ga_3$ film is shown in Fig. (4). The analysis of the X-ray diffraction for crystallized films showed that AsTe and GaTe phases coexist in the crystallized $As_{30}Te_{67}Ga_3$ film.

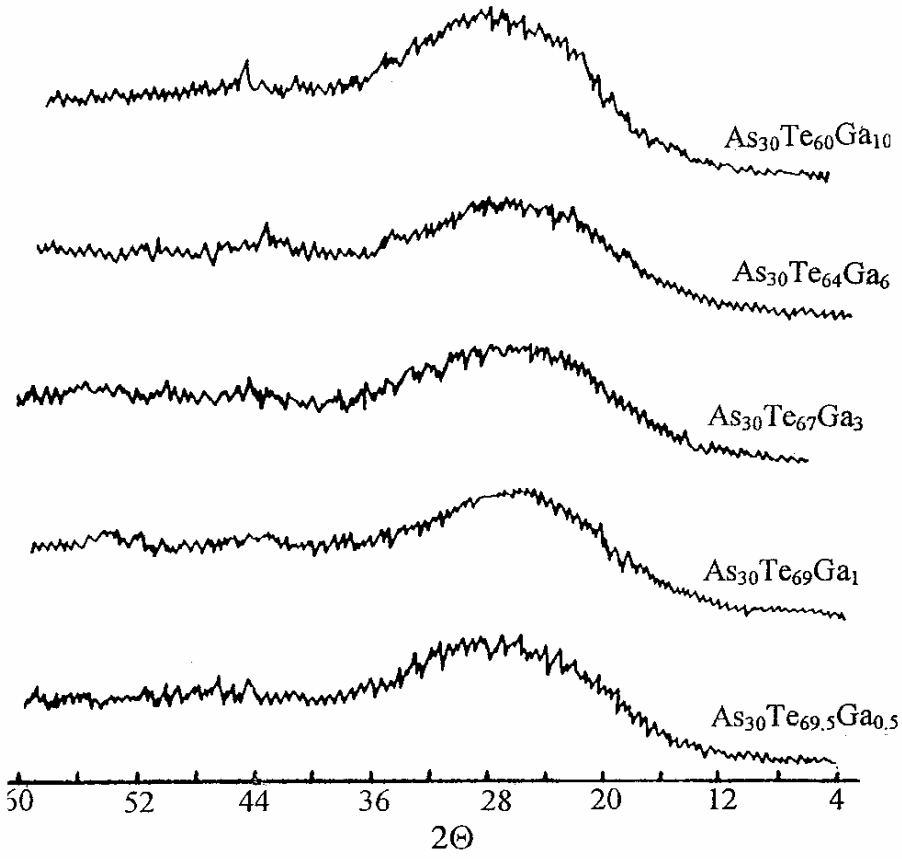

Fig.(3): The X-ray diffraction pattern for as-prepared As_{30} Te_{70-x} Ga_x films.

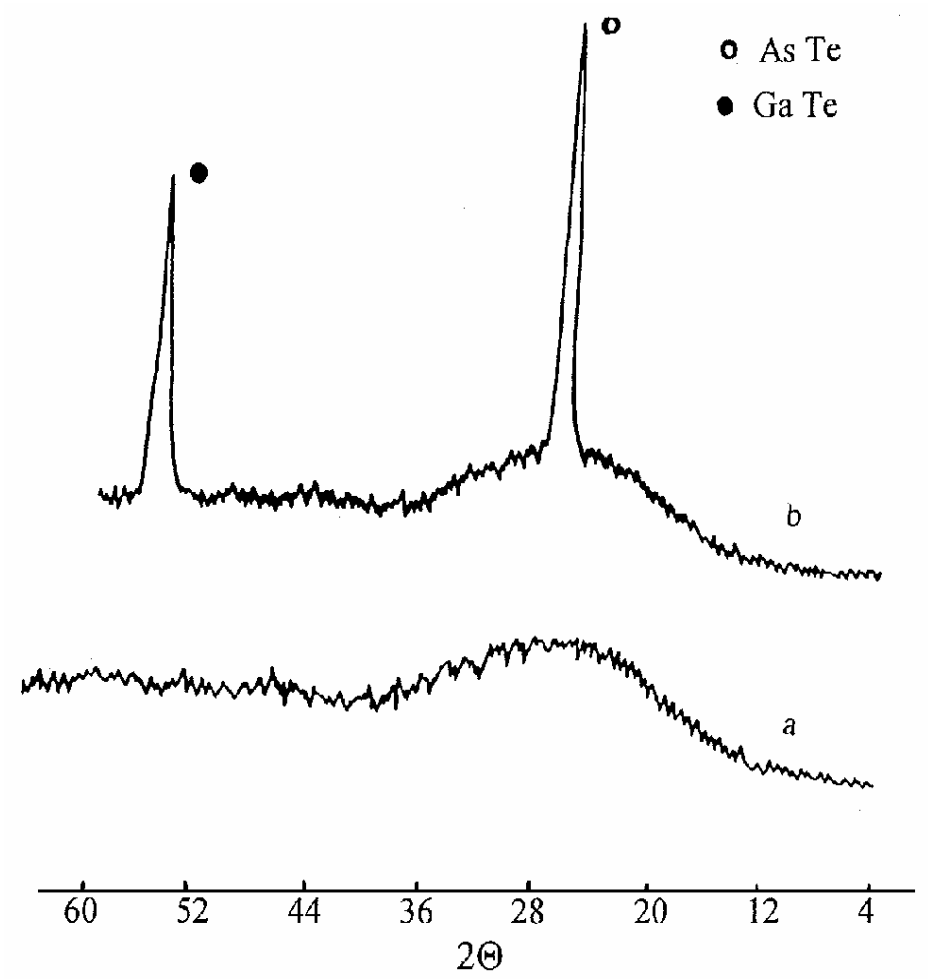

Fig. (4) X-ray diffraction pattern for As_{30} Te_{67} Ga_3 films
a) as-prepared
b) annealed at 423 K for 2hr

The selected area electron diffraction (SAED) for $As_{30}Te_{67}Ga_3$ film annealed at 453 K for 2hr is shown Fig. (5). The analysis of the SAED determines the most probable crystalline phases accompanied the transformations. The calibrated camera constant, obtained from the diffraction rings of standard element gold, was used to calculate the d-spacing corresponding to the different radii of the diffraction pattern. The results are summarized in Table (2) and in fairly good agreement with of d-spacing of

AsTe and, GaTe [3-4].

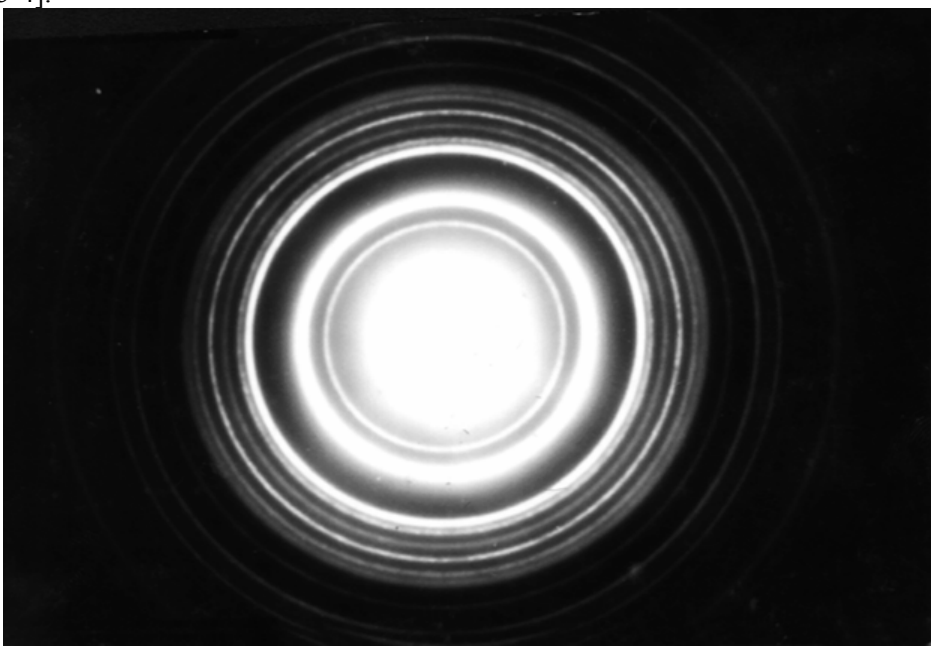

Fig.(5): The electron diffraction pattern for As_{30} Te_{67} Ga_3 film annealed at 453 K for 2 hr .

Table (2): Comparison of d-spacings (in Å) calculated from SAED with those observed on AsTe and GaTe [3.4] .

Present work	AsTe (after R. Quinn [3].	GaTe (after T. Wadsten [4] .
2.479		2.499
2.207		2.205
1.536	1.440	…….
1.442		…….
1.358	1.325	…….
1.261	1.291	……..
1.177	1.178	……..
1.039	1.020	……..
0.942	0.963	……
0.883	0.913	…….

It is known, that if the multiple reflections are neglected, the transmittance, T of the film is given by

$$T = (1-R)^2 \exp(-A) = (1-R)^2 \exp(-\alpha d) \quad (1)$$

where R is the reflectance, A is the absorbance, α is the absorption coefficient in cm^{-1}, and d is the film thickness. R can be determined from measurements of both T and A using Eqn.(1), which can be rewritten in the following form

$$R = 1 - \{T\exp(\alpha d)\}^{1/2} \quad (2)$$

The reflectance R of the material of refractive index, n and extinction coefficient, k is given by

$$R = \frac{(n-1)^2 + k^2}{(n+1)^2 + k^2} \quad (3)$$

The absorption coefficient α is related to k by

$$\alpha = 4\pi k/\lambda \quad (4)$$

where λ is the wavelength.

Using Eqs. (2), (4) and (3), the values of R, k, and n are calculated, respectively.

The fundamental absorption edge in most amorphous semiconductors follows the exponential law. In the high absorption region ($\alpha \geq 10^4$ cm^{-1}), the photon energy dependence of the absorption coefficient can be described by the quadratic relation[5]

$$(\alpha h\nu) = B\,(h\nu - E_o)^2 \quad (5)$$

where ν is the frequency of the incident beam, B is a constant and E_o is the optical gap.

Figure (6) shows the relation between $(\alpha h\nu)^{1/2}$ versus $(h\nu)$ for as-deposited $As_{30}Te_{70-x}Ga_x$ films of different compositions. The indirect optical energy gap can be obtained from the intercept of the resulting straight lines with the energy axis at $(\alpha h\nu)^{1/2} = 0$. The effect of Ga content on the indirect optical energy gap of as deposited $As_{30}Te_{70-x}Ga_x$ films, is shown in Fig. (7). The indirect optical energy gap has nearly constant value of 0.73 eV, up to x=3at.%, then the optical gap increases continuously with increasing Ga content and has a value of 0.9 eV for $As_{30}Te_{60}Ga_{10}$ film.

According to the Ga concentration, the relation of Fig. (7) is divided into two regions. In the first region, E_o is nearly independent on the Ga content, up to 3 at. %. In the second region where the Ga content > 3 at. %, E_o increases continuously with the increased Ga content. A similar results to that observed in the first region were reported for As-Te-In glasses by F. Kosek et al. [6], and for As-Te-Ag glasses by A. Giridhar et al. [7].Up to 3 at %, the Ga addition

acts as a dopant and it is uniformly dispersed in the As-Te glass network without affecting either the short range or the medium range ordering of the parent glass.

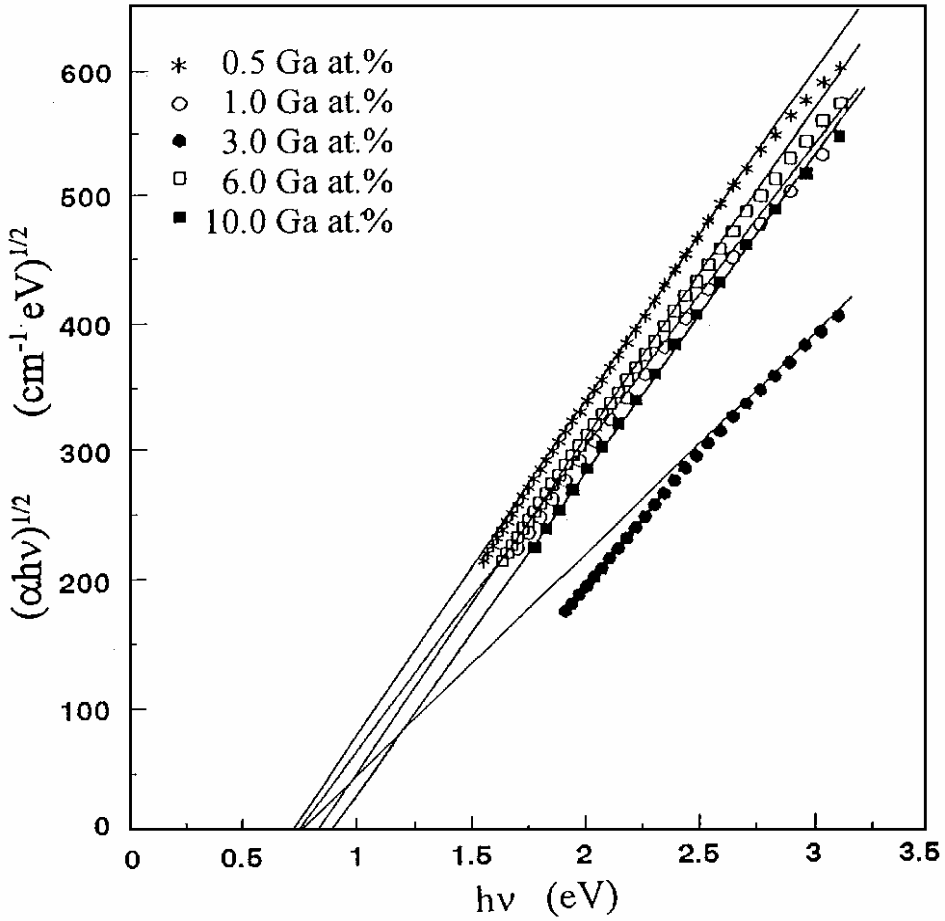

Fig.(6): A plot of $(\alpha h\nu)^{1/2}$ versus the photon energy hν, for as-prepared As_{30} Te_{70-x} Ga_x (with o.5 ≤ x ≥ 10 at.%) films.

The role of Ga as a dopant in the As-Te glass (Ga content from 0.5 to 3.0 at. %) is similar to those of metals such as Zn, Ga and In in As-Se glasses [6], where the dopants affect only the density of hopping sites near valance band edge, without affecting the charged densities of the mentioned defects in the amorphous semiconductor matrix.

In the second region, where the concentration of Ga is higher than 3 at.%, three component As-Te-Ga glasses are formed. For these compositions a monotonic increase of the optical energy gap with increasing the Ga content

was observed. At these Ga concentrations, the value of the optical energy gap will be evidentely determined by the energies and relative concentrations of the various types of bonds, which in turn determine the width of the valence and conduction bands as well as the location of the Fermi level.

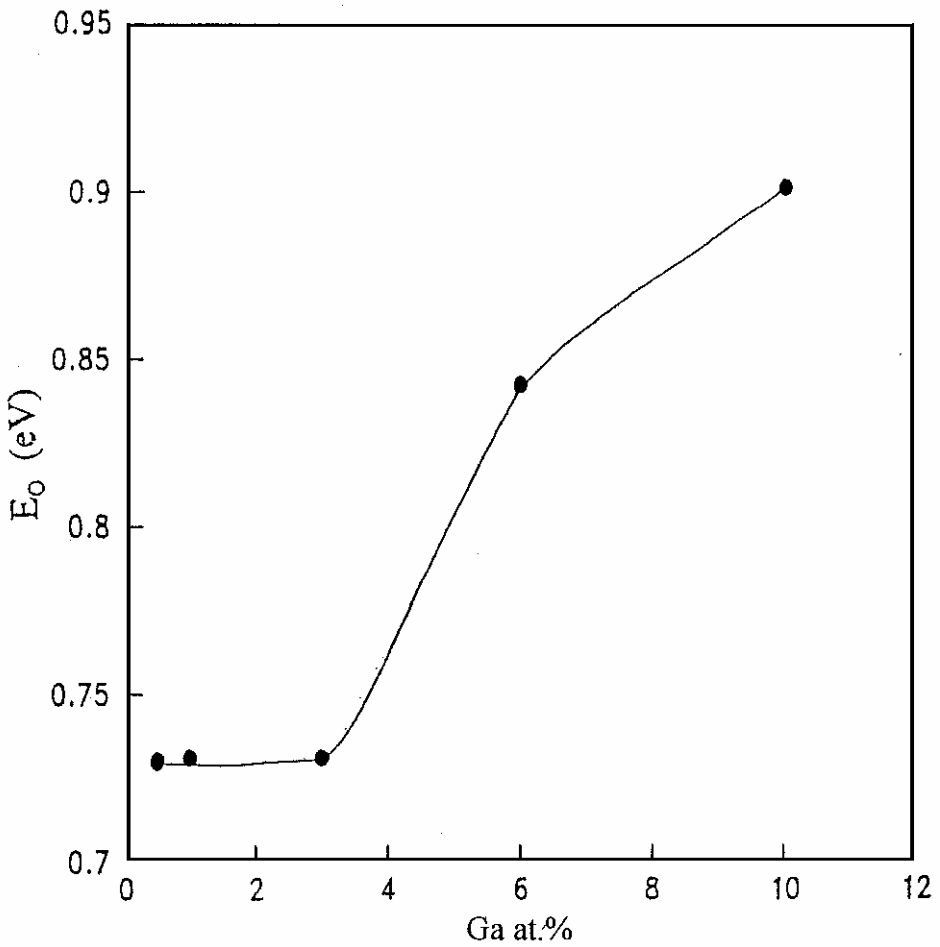

Fig.(7): The indirect optical energy gap(E_o) versus Ga content in for as-prepared $As_{30}Te_{70-x}Ga_x$ films .

The dependence of the refractive index, n on the wavelength (λ) for as-prepared $As_{30}Te_{70-x}Ga_x$ films, is shown in Fig. (8). It could be noticed that n decreases with increasing the wavelength to reach a constant value at λ longer than 900nm. The high frequency refractive index n_0, is estimated from extrapolation of the curves of Fig. (8). Table (3) shows the effect of composition of $As_{30}Te_{70-x}Ga_x$ films on the indirect optical energy gap (E_o) and the high frequency refractive index (n_0).

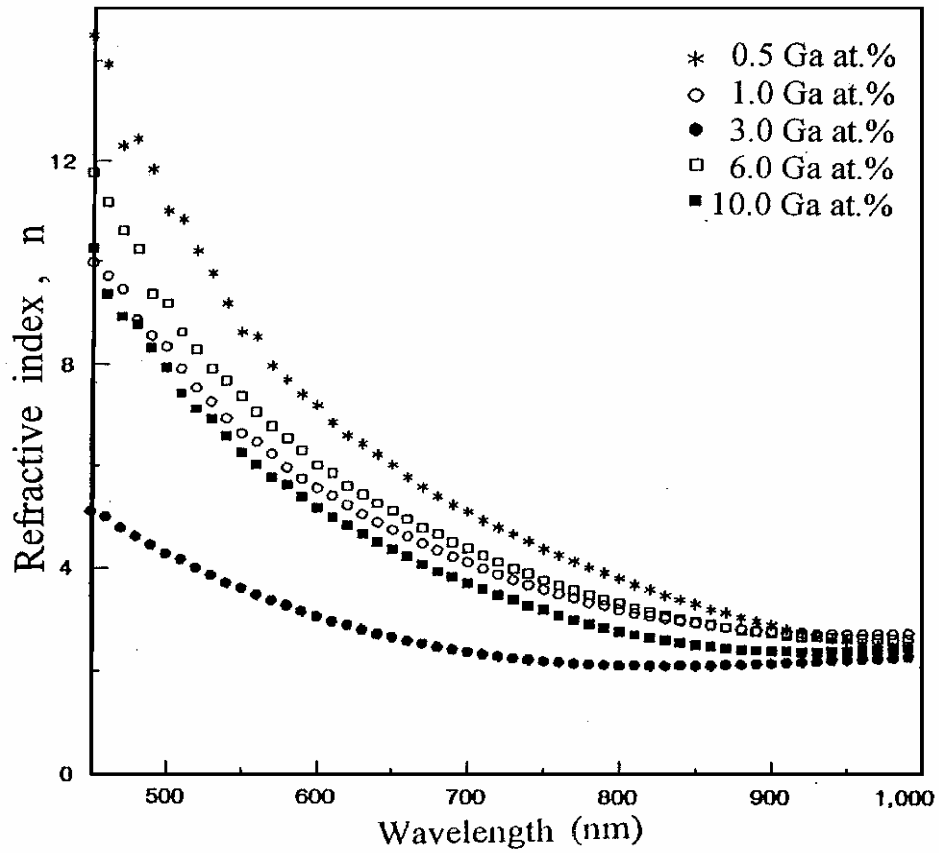

Fig.(8): The relation between refractive index (n) and photon wavelength for $As_{30}\ Te_{70-x}\ Ga_x$ films .

Table (3): The indirect energy gap (E_o) and the high frequency refractive index (n_o). at different values of Ga content.

Ga (at %)	E_o (eV)	n_o
0. 5	0.730	2.44
1	0.731	2.76
3	0.731	2.52
6	0.842	2.76
10	0.901	2.49

The dependence of the extenction coefficient(k)on the wavelength for as-prepared $As_{30}Te_{70-x}Ga_x$ films, is shown in Fig. (9). It could be noticed that k decreases linearly as photon wavelength increases followed by slight increase at wavelengths greater than 800nm.

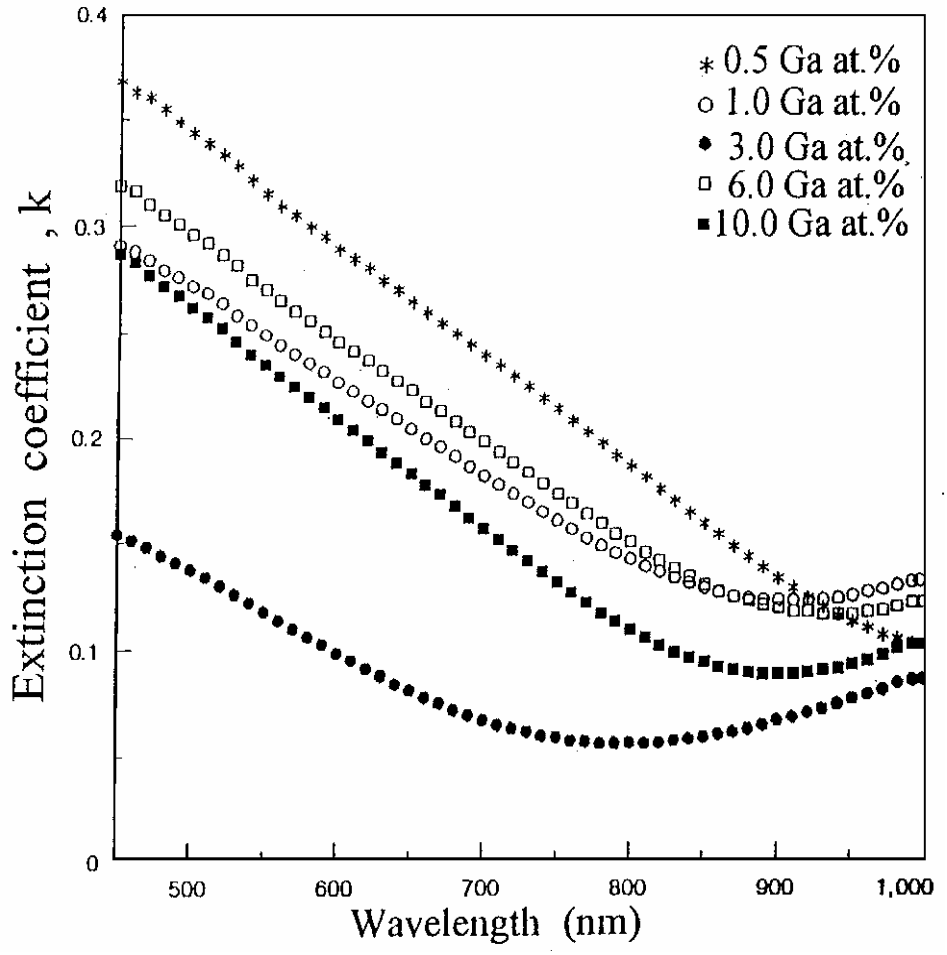

Fig. (9): The relation beween extenction coefficient (k) and the photon wavelength for As_{30} Te_{70-x} Ga_x films.

Figure (10) shows the variation of $(\alpha h\nu)^{1/2}$ with the photon energy ($h\nu$) for as-prepared and annealed $As_{30}Te_{67}$ Ga_3 films of thickness 2500Å. The dependence is linear and is extrapolated to $(\alpha h\nu)^{1/2} = 0$ to obtain the value of E_O. The effect of annealing temperature on the optical energy gap (E_O) for $As_{30}Te_{67}Ga_3$ (as a representative specimen of the studied $As_{30}Te_{70-x}Ga_x$ system) films, on the temperature range from 353K to 423K, is shown in Fig. (11). It could also be noticed that E_O increases slightly with increasing the annealing temperature up to 363 K, then decreases sharply with increasing the annealing temperature.

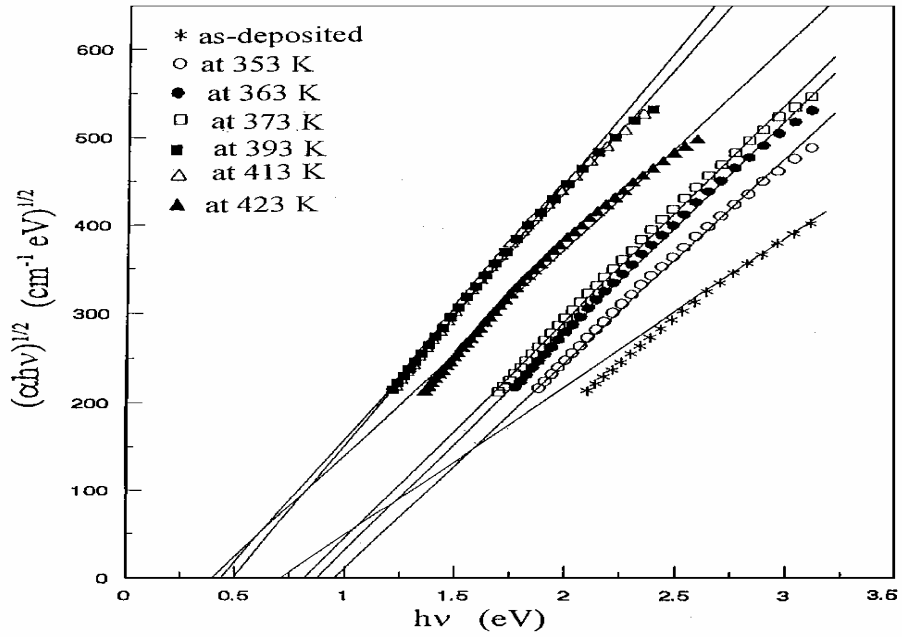

Fig.(10): A plot of $(\alpha h\nu)^{1/2}$ versus the photon energy hν, for as-prepared and annealed $As_{30}Te_{67}Ga_3$ films.

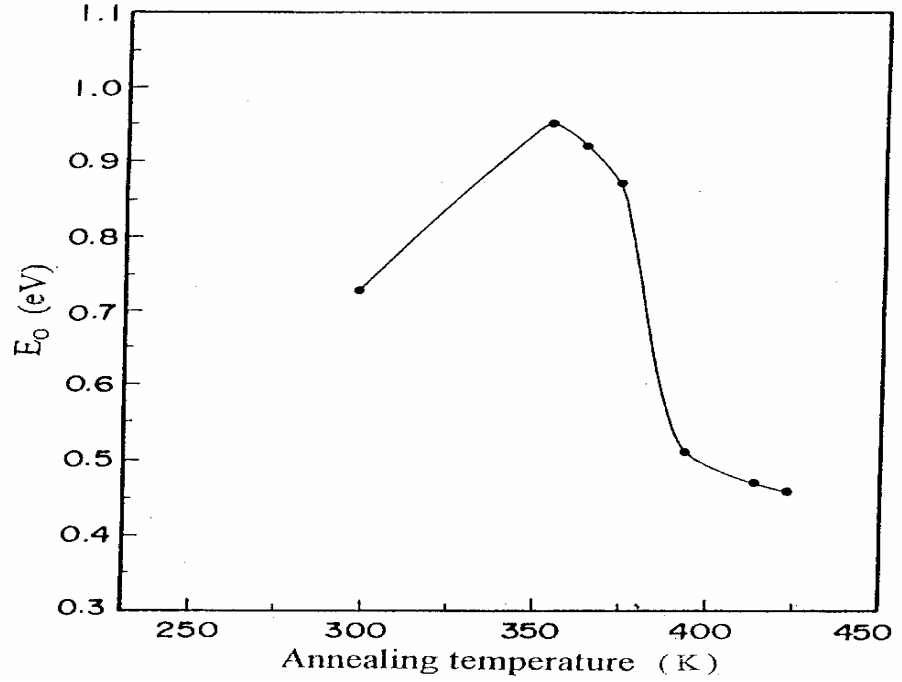

Fig.(11): The indirect optical energy gap as a function of the annealing temperature for As_{30} Te_{67} Ga_3 films.

The effect of thermal annealing on the optical energy gap could be divided into two regions, below and above the glass transition temperature. Annealing of $As_{30}Te_{70-x}Ga_x$ films at temperature below the glass transition temperature T_g slightly increased the value of the optical energy gap. The Fermi level in a chalcogenide is generally pinned near the middle of the gap giving information on the localized states in the gap [8]. The mobility gap is defined by E_o. [9]. The width of the localized states near the mobility edge E_C-E_A and E_B-E_V increase with increasing disorder in amorphous structure.

The variation of E_o can be explained by a shift of E_A and or E_B. The presence of high concentration of localized states in the band structure is responsible for the low value of E_o in the case of as-deposited amorphous films. During the thermal annealing, the unsaturated defects are gradually annealed out [10], producing large numbers of saturated bonds. The reduction in the number of unsaturated defects decreases the density of the localized states in the band structure, consequently increases the optical gap.

During the thermal annealing at temperature higher than T_g, enough vibrational energy is present to break some of the weaker bonds, thus introducing some translational degree of freedom to the system. These additional degree of freedom results in an increase in the film heat capacity. So, crystallization via nucleation and growth becomes possible and the amount of crystalline phases depends on the annealing temperature. The amount and type of separated polycrystalline phases depend on the original composition of the film and the annealing temperature. The continuous decrease of the optical energy gap with increasing the annealing temperature could be attributed to the phase separation of the crystalline phases.

Conclusion:

The as-deposited films of different compositions were amorphous and both T_g, and T_c increase with increasing Ga content. As the annealing temperature was increased above T_g, the thermally induced crystalline phases of AsTe and GaTe were formed. The indirect optical gap E_o has nearly constant value of 0.73 eV for $As_{30}Te_{70-x}Ga_x$ films, where x = 0.5-3 at.%, then it increases continuously with increasing Ga content and it has a value of 0.9 eV at x = 10 at.%. Thermal annealing at $T < T_g$ is accompanied by increasing of E_o. The results were discussed by Mott and Davis model. Annealing at $T > T_g$ was found to decrease E_o. The results were discussed via the amorphous-crystalline transformations.

References:

1. N.F. Mott, *Philos. Mag.* **19**, 835 (1969).

2. A.A. Dunaev, Z.U. Borisiva M.D. Mikhailov and I.V. Privalova, *Fiz. Kim, Stekla* **43**, 346 (1978).

3. R. Quinn, *Mater Res. Bull.* **9,** 803 (1974).

4. T. Wadsten, Chem. Commun., Univ. Stochholm, **10**, 1 (1985).

5. E.A. Davis and N.F. Mott, *Phil. Mag.* **22**, 903 (1970).

6. F. Kosek, Z. Cimpl, M.D. Mikhailov and E.A Karpova, *J. Non-Cryst. Solids* **86,** 265 (1986).

7. A. Giridhar and Sudha Mahadevan, *J. Non -Cryst. Solid* **197**, 228 (1996).

8. Y. Watenable, S. Kaneko, H. Kawazoe and M. Yamada, *Phys. Rev.* **B40**, 3133 (1989).

9. N.F. Mott, and E.A. Davis: "Electronic Processes in Non-Crystalline Material" (Clarndon Press Oxford), Chap. 7, (1971)

10. S. Hasegawa, S. Yazalci and T. Shimizu, *Solid State Commun*. **26**, 407 (1978).